

High Frame Rate Contrast-Enhanced Ultrasound for Velocimetry in the Human Abdominal Aorta

Voorneveld, J.; Engelhard, S.; Vos, H. J.; Reijnen, M. M.J.; Gijssen, F.; Versluis, M.; Jebbink, E. Groot; de Jong, N.; Bosch, J. G.

DOI

[10.1109/TUFFC.2018.2846416](https://doi.org/10.1109/TUFFC.2018.2846416)

Publication date

2018

Document Version

Accepted author manuscript

Published in

IEEE Transactions on Ultrasonics, Ferroelectrics, and Frequency Control

Citation (APA)

Voorneveld, J., Engelhard, S., Vos, H. J., Reijnen, M. M. J., Gijssen, F., Versluis, M., Jebbink, E. G., de Jong, N., & Bosch, J. G. (2018). High Frame Rate Contrast-Enhanced Ultrasound for Velocimetry in the Human Abdominal Aorta. *IEEE Transactions on Ultrasonics, Ferroelectrics, and Frequency Control*, Article TUFFC-08671-2017. <https://doi.org/10.1109/TUFFC.2018.2846416>

Important note

To cite this publication, please use the final published version (if applicable).
Please check the document version above.

Copyright

Other than for strictly personal use, it is not permitted to download, forward or distribute the text or part of it, without the consent of the author(s) and/or copyright holder(s), unless the work is under an open content license such as Creative Commons.

Takedown policy

Please contact us and provide details if you believe this document breaches copyrights.
We will remove access to the work immediately and investigate your claim.

High Frame Rate Contrast-Enhanced Ultrasound for Velocimetry in the Human Abdominal Aorta

J. Voorneveld, *Student Member, IEEE*, S. Engelhard, H.J. Vos, *Member, IEEE*, M.M.P.J. Reijnen, F. Gijssen, M. Versluis, *Member, IEEE*, E. Groot Jebbink, N. de Jong, *Associate Member, IEEE*, and J.G. Bosch, *Member, IEEE*

Abstract— Treatment of abdominal aortic (AA) aneurysms and stenotic lesions may be improved by analyzing their associated blood flow patterns. Angle-independent blood flow patterns in the AA can be obtained by combining echo-particle image velocimetry (ePIV) with high frame rate contrast-enhanced ultrasonography. However, ePIV performance is affected by ultrasound contrast agent (UCA) concentration, microbubble stability and tissue clutter. In this study we assessed the influence of acoustic pressure and UCA concentration on image quality for ePIV analysis. We also compared amplitude modulation (AM) and singular value decomposition (SVD) as tissue suppression strategies for ePIV. Fourteen healthy volunteers were imaged in the region of the distal AA. We tested four different UCA bolus volumes (0.25, 0.5, 0.75 and 1.5 ml) and four different acoustic output pressures (mechanical indices: 0.01, 0.03, 0.06 and 0.09). As image quality metrics, we measured contrast-to-background ratio, bubble disruption ratio and maximum normalized cross-correlation value during ePIV. At mechanical indices ≥ 0.06 , we detected severe bubble destruction, suggesting that very low acoustic pressures should be used for ePIV. SVD was able to suppress tissue clutter better than AM. The maximum tracking correlation was affected by both UCA concentration and flow rate, where at high flow rates, lower UCA concentrations resulted in slightly higher correlation values but more signal drop-outs during late diastole. High frame rate ePIV was successfully performed in the AA of healthy volunteers and shows promise for future studies in patients.

Index Terms— abdominal aorta, echography, echo-particle image velocimetry, ePIV, high frame rate ultrasound, vascular flow, ultrasound contrast agents

I. INTRODUCTION

Study of abdominal aortic (AA) flow patterns may assist the disease-progression prediction process in patients with AA stenotic lesions and aneurysms. Several studies on stenotic lesions suggest that local flow patterns and their associated flow parameters, such as wall shear stress, have an influence on lesion development and progression [1]–[3]. In AA aneurysms, changes in flow patterns modulate inflammatory mechanisms in the vascular endothelium, causing aneurysm growth [4]. For AA aneurysms and stenotic lesions around the aortic bifurcation, *in vitro* data have shown that different treatment options generate different flow perturbations [5], [6], which can partly explain the different outcomes of these treatments. Post-treatment analysis of AA blood-flow patterns may make the follow-up schemes after endovascular treatment more patient-specific by predicting potential failure.

Investigation of blood flow patterns *in vivo* requires full field, angle independent velocity measurements. Currently, the most widely used method of assessing AA blood flow is Doppler ultrasound. However, conventional Doppler is angle dependent, which complicates imaging blood flow in regions of bifurcation, where blood flows in different directions, and where it can also flow approximately perpendicular to the ultrasound beam (70° to 110°) [7], [8].

Several ultrasonic techniques have been developed to overcome the angle dependency limitations of standard Doppler. *Vector Doppler Imaging* (VDI) splits the transmit aperture, obtaining multiple Doppler measurements at known angles to each other, from which both velocity magnitude and direction can be deduced [9], [10]. However, for imaging of deep structures, the angles between beams, and hence velocity estimates, can become unreliable due to the limited aperture [11]. *Transverse Oscillation* is a technique that also utilizes a split aperture, although usually only synthetically in receive [12]. Although originally limited to linear arrays, this method has recently been expanded to work with curved arrays, being demonstrated in the portal vein of a healthy volunteer [13]. However, the velocities expected in the AA are much higher

This work was supported in part by ZonMw within the Innovative Medical Devices Initiative (IMDI) program (project Heart Failure and 4D Flow, project number 104003001).

J. Voorneveld, H.J. Vos, F. Gijssen, N. de Jong and J.G. Bosch are with the Department of Biomedical Engineering, Thorax Center, Erasmus MC, Rotterdam, The Netherlands.

S. Engelhard, M. Reijnen and E. Groot Jebbink are with the Department of Vascular Surgery, Rijnstate Hospital, Arnhem, The Netherlands.

E. Groot Jebbink and M. Versluis are with the Physics of Fluids group, MIRA Institute for Biomedical Technology and Technical Medicine, University of Twente, Enschede, The Netherlands.

N. de Jong and H.J. Vos are also with the Department of Imaging Physics, Faculty of Applied Sciences, Delft University of Technology, Delft, The Netherlands.

than those in the portal vein. *Blood Speckle Tracking* can obtain angle-independent velocity measurements by tracking the speckle motion of moving red blood cells between frames [14]. It, however, requires sufficient temporal resolution for tracking the range of flows expected in the AA. High frame rate (HFR) imaging, using unfocussed transmissions, allows for the temporal resolution required for tracking high blood flow velocities, but is complicated by strong clutter in the blood-pool from surrounding tissue and reduced penetration depth compared to focused transmissions [15].

Echo-particle imaging velocimetry (ePIV) using ultrasound contrast agent (UCA) can be beneficial for the penetration depths required in AA flow imaging in patients (6-10 cm), since backscattered signal is greatly improved over native blood cells. We have shown previously that HFR ePIV can accurately measure the high velocity flows which are expected in the AA, *in vitro* [16]. Translation to *in vivo*, however, requires further optimization of critical UCA related parameters, such as mechanical index (MI), UCA concentration and the applied tissue suppression strategy.

UCA specific acquisition sequences suppress tissue signal by exploiting the non-linear behavior of UCA, e.g. amplitude modulation (AM) or pulse inversion. However, these sequences incur a cost in frame rate, as multiple transmissions are required to reconstruct a single image. Alternatively, singular value decomposition (SVD) based tissue suppression has been shown to perform equivalently or better than UCA specific acquisition sequences, although only for microvascular flow environments [17]. It is not yet known whether SVD also performs well in large vessels like the abdominal aorta.

The use of UCA also mandates careful tuning of the acoustic pressures used for imaging. Too-low pressures may generate insufficient signal from the bubbles; while overly-high pressures can result in bubble destruction. In both cases, velocity estimation will be compromised. The relationship between acoustic pressure and bubble destruction during HFR imaging has been reported only for *in vitro* studies [18]–[20]. It is well known that bubble stability is affected by physiological conditions. In this study we assess bubble destruction *in vivo*.

Another variable requiring optimization is UCA concentration. Higher concentrations are associated with higher signal power, but may reduce ePIV accuracy if too high [21], [22]. Conversely, low concentrations may leave void regions, occupied only by noise. The effect of UCA concentration has not yet been studied for HFR ePIV.

In this study, we investigate the effect that tissue suppression strategy (AM versus SVD), acoustic pressure and UCA concentration have on image quality metrics for ePIV, in human volunteers.

II. METHODS

A. Study Design

After approval as a pilot study, by the medical ethic committee of the Erasmus Medical Center (NL58025.078.16), 15 healthy volunteers (age 18-35 years, BMI <25) were imaged in the region of the distal aorta with the aortic bifurcation and proximal iliac vessels in a coronal view. Four bolus injections of UCA (0.25, 0.5, 0.75 and 1.5 ml, SonoVue, Bracco S.p.A., Milano, Italy) were administered before acquiring 2.5 s of HFR ultrasound data with a research ultrasound system (Vantage 256, Verasonics Inc., Kirkland WA, USA).

An additional clinical ultrasound system (Epiq 7, Philips Healthcare, Andover, MA, USA) was used to simultaneously record contrast mode image sequences in the left superficial femoral artery (downstream of the AA). HFR recordings in the AA were initiated on the research ultrasound system once the bolus was detected in the femoral artery.

After imaging the first volunteer, some minor adjustments/improvements were made to the acquisition scheme, making the data of this volunteer incomparable with the others. Measurements were performed on the remaining 14 volunteers during four measurement sessions (afternoons) in groups of 3-4.

The first three volunteers were imaged at a transmit voltage of 30V. Due to clearly visible bubble destruction on the clinical system, the transmit voltage on the Verasonics ultrasound system was decreased for subsequent volunteers, after each measurement session. Thus, three volunteers were imaged using a transmit voltage of 30V, three at 20V, four at 10V and four at 5V. The transmit voltages of 30V, 20V, 10V and 5V correspond to MIs of 0.09, 0.06, 0.03 and 0.013, respectively (at a depth of 30-50 mm taking into account a tissue attenuation of -0.3 dB per cm).

Additionally, the volunteers underwent MRI phase contrast imaging and the detected flow was compared to the ePIV results. This part of the study is not further described here, but reported elsewhere [23].

B. Ultrasound Acquisition and Image Reconstruction

RF data were acquired with a curvilinear probe (3 MHz, C5-2, ATL, Bothell WA, USA) connected to the research ultrasound system. The AM sequence consisted of diverging waves (transmit delays all zero, single cycle pulse) transmitted with different apodization schemes (even, full, and odd elements active [24], [25]) at a pulse repetition frequency (PRF) of 3000 Hz. The sum of odd and even apodization transmissions was coherently subtracted from the full transmit to produce AM images at 1000 fps. From the full transmit acquisitions a standard B-mode sequence of 1000 fps was also generated, producing synchronized datasets for comparison. Images were beamformed into the polar domain where further analysis was performed.

C. Singular Value Decomposition (SVD)

SVD based clutter suppression assumes that the tissue, blood and noise components of an image sequence can be separated based on their respective spatiotemporal coherence energy [26]. Tissue signal is typically higher intensity and more spatiotemporally coherent than flowing blood (and bubble) signal. Thus, when an image sequence containing blood flow and surrounding tissue is decomposed using SVD, the tissue signal accumulates more coherence energy than the flowing blood. This causes tissue to collect in the low-rank modes of the system while blood and bubbles are distributed more centrally (Fig 1.). Noise, being relatively incoherent and low intensity, typically resides in the high-order modes. Truncating low and/or high order modes allows for selective removal of tissue and/or noise from the image sequence.

In this study, a low-rank threshold selection algorithm was used to automatically detect the transition between tissue and flowing UCA. Low-rank selection was based on the ratio of successive singular values: $\sigma_n/\sigma_{n-1} > 0.99$ (see Fig. 1). This criterion selects the first mode n which decreases less than 1% in energy from its predecessor [27]. A high-rank cutoff was not used in this study.

The number of frames used when performing SVD (ensemble length) is known to affect the separability of slow moving bubbles and tissue [17]. Thus, to assess the effect of SVD ensemble length on contrast-to-background ratio (CBR) four different SVD ensemble lengths were tested: 32, 64, 128 and 1250 frames (all frames). CBR was assessed during periods of slow flow (velocity magnitude < 0.1 m/s) and fast flow (velocity magnitude > 0.4 m/s) separately. Comparison was performed on data with MI = 0.01 only to reduce the influence of bubble disruption on the comparison.

SVD was performed on beamformed IQ data. For ensemble lengths of 32, 64 and 128, individual SVD outputs needed to be combined into a continuous set of frames. Thus, ensembles were overlapped by 87.5%, where overlapping frames from different SVD ensembles were averaged to create the final SVD outputs. This was not required with the 1250 ensemble as only one SVD output was created.

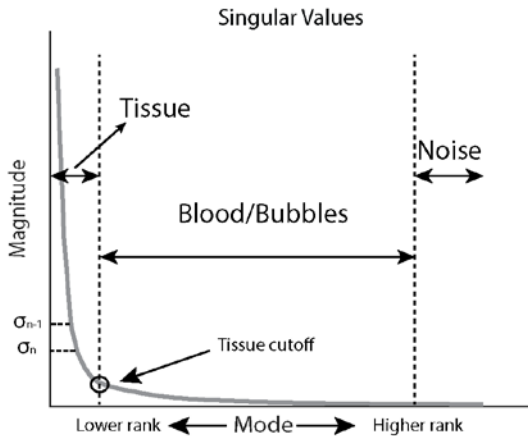


Fig. 1. Illustration of the low-rank threshold selection algorithm used in this study. Tissue cutoff is found by searching for the point in the curve where the slope begins ‘flattening out’.

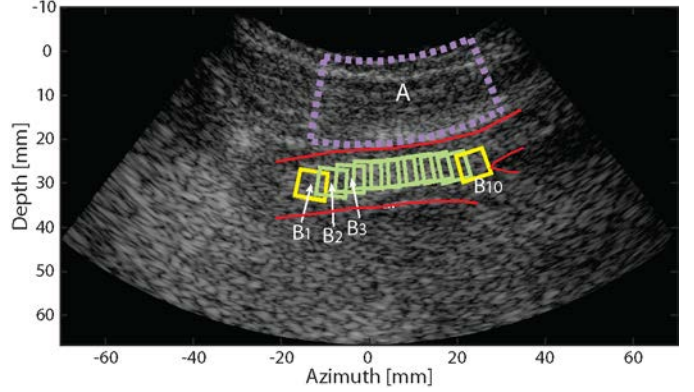


Fig. 2. Regions used for calculating DR and CBR. Red lines indicate outlines of AA and bifurcation of iliac arteries. Purple dotted region A was used for tissue signal strength. Regions B1 to B10 were used for UCA signal strength. B1 and B10 were used for DR. Images displayed at 50dB dynamic range.

D. Tissue Suppression Strategies

AM was compared to SVD (ensemble length = 1250 frames) as a method for suppressing tissue signal without deteriorating the UCA signal. SVD images were computed from the B-mode sequences. Additionally, a 2nd order Chebyshev high-pass filter with a -6dB cut-off at 15 Hz was applied to the AM data, acting as a low-cut-off frequency Doppler wall-filter (AM+Cheby). SVD was also applied to the AM processed data (ensemble length = 1250 frames) as an additional group for comparison (AM+SVD), to investigate the usefulness of a combination of the two techniques.

E. Contrast-to-Background Ratio (CBR)

Tissue suppression efficacy was assessed using contrast-to-background ratio (CBR) [28], defined as $CBR = 10 \log_{10}(\overline{RMS}_{B_{1-10}}/\overline{RMS}_A)^2$, where \overline{RMS} is the time-averaged root-mean-square signal strength in UCA (Fig. 3: **B**₁₋₁₀) and tissue regions (Fig. 3: **A**). Comparison between AM and SVD was performed during periods of slow flow (mean velocity < 0.1 m/s), which is the worst-case scenario for SVD, where bubble coherence between frames is similar to that of slowly moving tissue, increasing the likelihood that bubble signal will be removed along with the tissue signal

F. Disruption Ratio

UCA disruption ratio (DR), a measure of acoustically driven bubble destruction, was calculated as $DR = 1 - \overline{RMS}_{B_{10}}/\overline{RMS}_{B_1}$, where \overline{RMS} is the time-averaged RMS signal in the proximal (Fig. 3:**B**₁) and distal (Fig. 3:**B**₁₀) regions inside the AA. DR values range from 0 to 1, implying not any and full bubble destruction, respectively [20]. DR was calculated on the SVD processed datasets during systole only (mean velocity > 0.4 m/s) to ensure that fresh bubbles were being supplied to the region of interest.

G. Bubble Concentration / Velocity Tracking

This section describes how the velocity and correlation values were calculated for comparison between different bolus concentrations. Velocity in the center of the vessel was

estimated using normalized cross-correlation (along slow-time, frequency domain implementation) in ten regions (Fig 3: **B₁₋₁₀**) running along the length of the vessel. Each region was 4.7° by 6 mm in size, resulting in regions sized approximately 6 mm by 6mm, once scan converted. This size was chosen to meet the widely accepted ¼ interrogation window rule for PIV [29]. Normalized cross-correlation was performed on the polar beamformed data after envelope detection. The maximum correlation value was used as a measure of tracking performance for different UCA concentrations. Velocity vectors were determined by finding the location of maximum cross-correlation per region (Fig 3. **B₁₋₁₀**). Subpixel displacement was estimated using the centroid approach [29]. Velocity vectors were scan-converted and then smoothed using a temporal moving median filter (15 ensemble length). Bubble concentrations during diastolic (mean velocity < 0.1 m/s) and systolic (mean velocity > 0.4 m/s) phases were assessed separately, where maximum normalized cross-correlation and CBR were used for comparison.

H. ePIV Measurement

A full ePIV measurement is demonstrated on a volunteer imaged at 0.01 MI with a bolus volume of 1.5 ml, after applying a 1250 ensemble SVD filter. Four cross-correlation iterations were performed with window deformation, using interrogation areas of 9.5° x 6.1 mm and an overlap of 75% [29]. Correlation compounding was performed on three subsequent frame pairs before subpixel displacement estimation using a centroid approximation [29]. Vector fields were processed for display - at peak systole, backflow and diastole - using the dynamic visualization procedure described in [30]. Vessel boundaries were manually segmented.

I. Statistics and Reporting

Significance of differences was statistically tested using a two-tailed Student's t-test, where a p-value < 0.05 implied significance. Results are reported as mean ± standard deviation.

For box plots: circles denote individual data points; whiskers extend to max and min values of non-outliers; boxes start and stop at first and third quartiles; solid lines denote median; and dashed lines denote mean (if present).

III. RESULTS

Ultrasound contrast agent (UCA) was detected in all volunteers using HFR ultrasonography with no adverse events. UCA signal could be detected using all of the tissue suppression strategies tested.

A. SVD Ensemble Length

Increasing SVD ensemble lengths resulted in increasing CBR during periods of slow flow (Fig. 3). However, during periods of fast flow shorter ensembles resulted in higher CBR.

B. Mechanical Index (MI)

For AM processed data, increasing MI resulted in reduced CBR (Fig. 4.a). Larger bolus volumes resulted in higher CBR

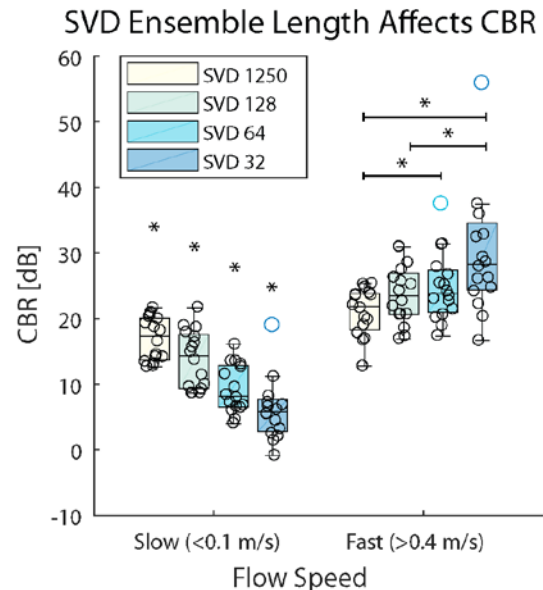


Fig. 3. CBR values obtained with different SVD ensemble lengths during periods of slow and fast flow. Longer ensembles achieve higher CBR during slow flow. During fast flow, the opposite is true. Only 0.01 MI data was used for this comparison. n = 16 (volunteers x bolus volumes). * p < 0.05

but only for the lower MIs (0.01 and 0.02 - Fig 4.a). The tissue signal after AM processing increased quadratically with increasing MI (Fig 4.b). Higher MIs (0.06 and 0.09) caused considerably more microbubble destruction than lower MIs (Fig. 4.c). Contrast-ultrasound recordings in the femoral artery, downstream from the HFR imaged AA, showed dips in intensity during HFR insonification for the higher MIs but not for the lower MIs (Fig. 5).

C. Tissue Suppression

SVD consistently provided superior CBR values to AM and filtered derivatives of it, for all the MIs tested (Fig. 6). No significant differences were noted between AM+Cheby or AM+SVD, although both resulted in higher CBR than AM alone, even at 0.01 MI, where AM performed at its best. Frames of each filter group at different MIs are shown during slow flow only ($|v| < 0.1\text{ m/s}$) in Fig. 7. The average depth to the centerline of the aorta observed in these volunteers was $32 \pm 5\text{ mm}$.

D. Bubble Concentration

Correlation between frames during fast flow (0.3 ± 0.05) was weaker than during slow flow, independent of UCA concentration (0.7 ± 0.1 , Fig. 8.a). The 0.25 ml bolus had a lower correlation during slow flow than the 1.5 ml bolus (0.65 ± 0.14 vs. 0.79 ± 0.05 , $p=0.03$) but a higher correlation during fast flow (0.35 ± 0.04 vs. 0.30 ± 0.02 , $p=0.007$). Larger bolus volumes increased CBR for both diastolic and systolic flow rates (Fig. 8b), where systolic CBR was higher than diastolic on average ($23 \pm 5\text{ dB}$ vs $18 \pm 5\text{ dB}$, respectively, $p < 0.001$). For the 0.25 ml bolus volumes, signal 'drop-outs' were observed towards the end of diastole, where bubble signal was

lost in small regions. This was less prominent in higher concentrations.

E. ePIV Measurement

Taking into account the optimization described in previous sections, ePIV vector-fields were derived from a volunteer with an MI of 0.01 and a UCA bolus of 1.5ml. The results are shown in Fig 9.

IV. DISCUSSION

High frame rate contrast enhanced ultrasonography was successfully performed in the abdominal aorta of healthy volunteers. Velocity field information could be determined using ePIV (with the optimization described in this study) which was very similar to 4D phase-contrast magnetic resonance imaging [23].

A. SVD Ensemble Length

Longer ensemble lengths resulted in increased sensitivity to slow moving bubbles. This was expected as using more frames allows for more time for slow-moving bubbles to develop differences in spatial-temporal coherence from the slow-moving tissue. We also observed that shorter ensemble lengths resulted in higher CBR values for fast flow; this may be due to shorter ensembles being able to remove the pulsatile motion of the vessel wall better than long ensembles.

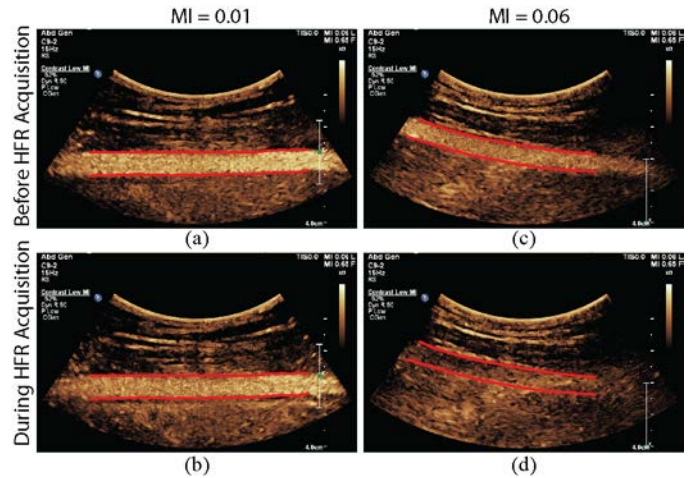


Fig. 5. Contrast mode images recorded downstream from the abdominal aorta, in the left superficial femoral artery with a clinical ultrasound system. Images are recorded a few seconds before (a, c) and during (b, d) the high frame rate (HFR) acquisitions in the abdominal aorta, for MIs of 0.01 (a, b) and 0.06 (c, d). For 0.06 MI, note the dramatic reduction in contrast intensity before (c) and during (d) the HFR acquisition. This is not the case of 0.01 MI, where contrast intensities before (a) and during (b) HFR acquisition are very similar.

However, for AA applications longer ensemble lengths are preferable as their CBR is best during slow flow and sufficient during fast flow.

B. Mechanical Index (MI)

1) Contrast-to-Background Ratio (CBR)

Lower MIs resulted in higher CBR values for AM processing (Fig 4.a). The reason is two-fold: 1) higher MI results in more bubble destruction (Fig. 4.b); and 2) higher MI accompanied higher tissue signal (Fig. 4.c), even after removal of the linear signal component. The reason for the increased tissue intensity is likely non-linear propagation of the pressure wave through tissue, which increases quadratically with the ultrasonic pressure applied [31]. We also observed apparent bubble signal below the AA (Fig. 7), possibly caused by non-linear

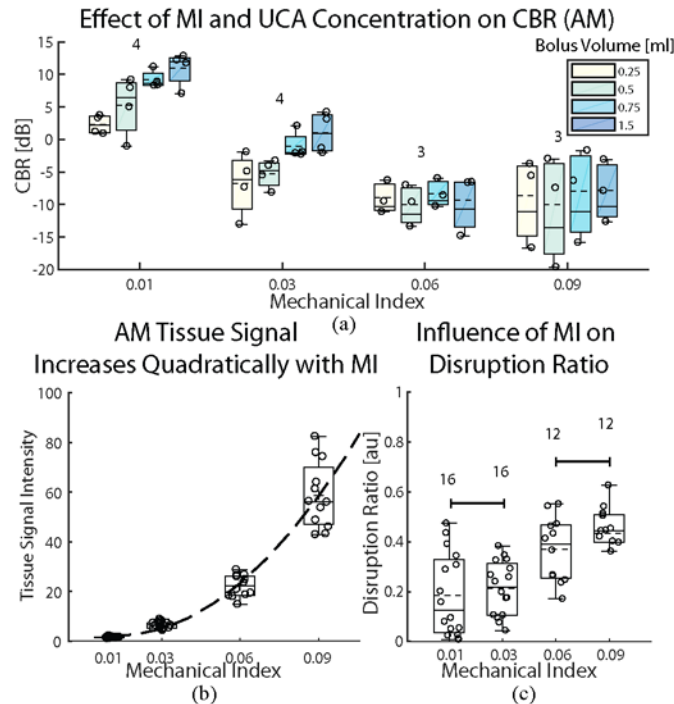


Fig. 4. Effects of MI on CBR of AM images and DR. a) Increasing MI results in lower CBR for AM processing. At $MI \leq 0.03$ larger bolus volumes result in more CBR. b) Tissue-signal intensity after AM processing increases quadratically with MI (dashed line indicates quadratic fit). c) Increasing MI results in more bubble destruction, where horizontal bars denote non-significant differences between groups. Numbers represent sample size (volunteers x bolus volumes).

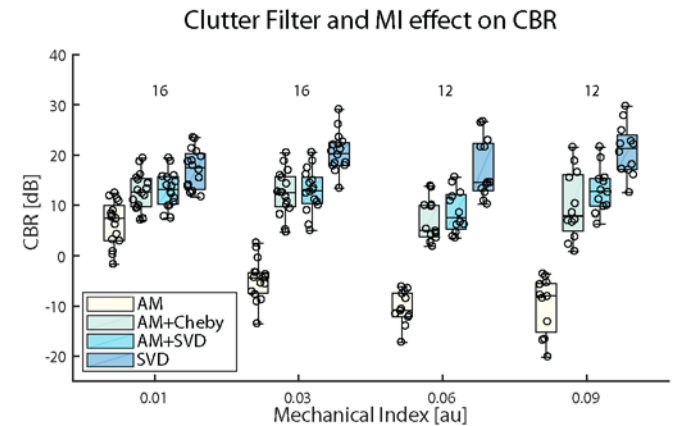


Fig. 6. CBR values for increasing MI and different contrast enhancement schemes (clutter filters). SVD is consistently superior to AM, AM+Cheby and AM+SVD. Note that while AM CBR reduces with increasing MI, AM+Cheby and AM+SVD do not. CBR calculated during periods of slow flow only (velocity < 0.1 m/s). Numbers represent sample sizes (volunteers x bolus volumes).

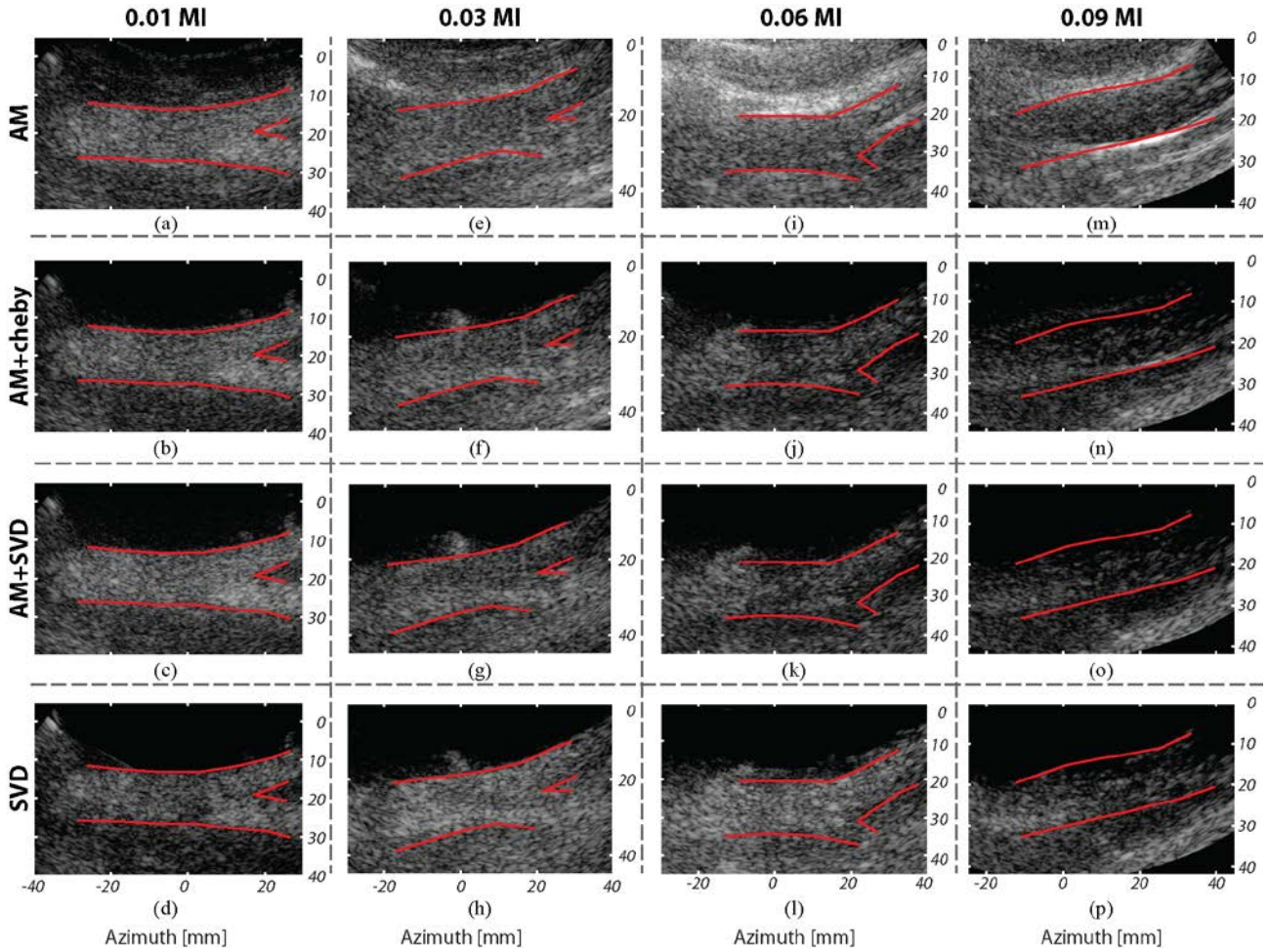


Fig. 7. AM, AM+Cheby, AM+SVD and SVD processed frames during slow diastolic flow (<10 cm/s) for the MIs studied (different volunteers). Bolus volume was 1.5 ml. Red lines indicate vessel boundaries. Higher MI results in higher AM tissue signal power and increased bubble destruction (left column to right column). SVD processing produces higher CBR than AM and its filtered derivatives. Images displayed at 50dB dynamic range and normalized individually.

propagation through the UCA filled AA, as described in [32], [33].

2) Disruption Ratio (DR)

We observed some differences in bubble destruction to those reported by *in vitro* studies. Couture *et al.* [18] reported more than 75% DR at peak-negative pressures of 0.2 MPa (\sim MI of 0.01 at 7.5 MHz), whereas we observed \sim 20% DR at a MI of 0.01. However, exposure time to ultrasound (\sim 80 ms here versus 25 s used in their study) and acoustic frequencies used (3 MHz versus 7.5 MHz) were drastically different between our two studies. To the contrary, Toulemonde *et al.* [20] observed negligible bubble destruction at a MI of 0.1. However, their MI values were measured close to the probe, whereas here (and in [18]) MI was measured at the depth of interest (30 mm here and 20mm in [18]). Finally, *in vitro* studies do not typically account for physiological temperatures [34]–[36] and pressures [37], gas exchange between blood and UCA [38], [39] or filtration by the lungs. We found that a maximum MI of 0.03 could be used without severe bubble destruction. However, it is important to note that DR was

established during periods of fast flow; during slow flow, the contrast bubbles will be exposed several times longer to ultrasound resulting in more severe bubble destruction in a given region. Therefore, the lowest MI is preferred. In further research, even lower MI values could be tested.

C. Amplitude Modulation vs. Singular Value Decomposition

SVD achieved higher CBR values than AM (Fig. 6 and Fig. 7). Even when combined with a very ‘mild’ wall filter (AM+Cheby), AM performed worse than SVD. We also tested how applying SVD to AM processed images would compare to SVD on a B-mode image. From Fig. 7c, it appears that AM+SVD provides higher signal intensities. However, Fig. 6 shows that SVD alone provides higher CBR values than AM+SVD. AM processing reduces the signal level and introduces additional noise during the coherent subtraction process of the AM sequence, which both deteriorate CBR.

Although SVD performed well on this data, with small amounts of non-rigid tissue motion, it may not perform so well

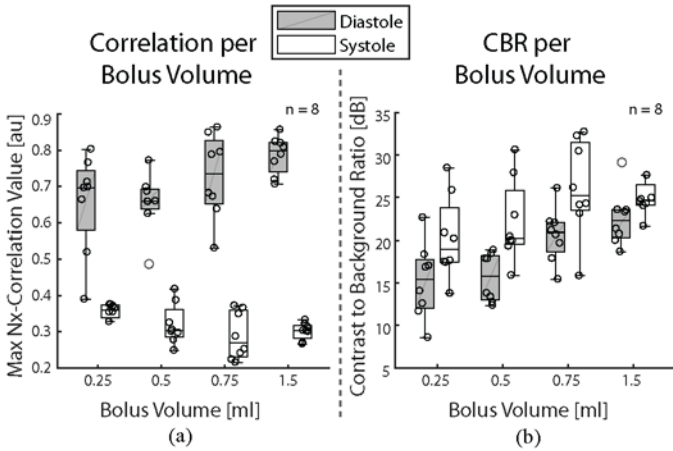


Fig. 8. Effect of increasing UCA concentration (bolus volume) on a) maximum normalized cross-correlation values and b) CBR. During fast flow, low concentrations result in slightly stronger correlation between frames than high concentrations. However, during periods of slow flow the opposite was true. Numbers represent sample sizes (number of volunteers).

where tissue motion is relatively large, e.g. the motion of the heart valves and wall in echocardiography.

CBR is not the only factor worth considering in the comparison between AM and SVD. AM needs at least two transmissions to produce an image; we implemented a commonly used three-transmission sequence which overcomes a limitation in the research ultrasound system to quickly switch between different transmit voltages. SVD can be applied to single transmission sequences, as performed in this study. Thus higher frame rates can be achieved when using SVD alone, or angular compounding can be used to reduce side-lobe levels, increasing both resolution and contrast [40]. However, it should be noted that coherent compounding of angular transmissions in the presence of fast moving scatterers is not straightforward, as decorrelation of the scatterers between different angles causes strong imaging artefacts [41]. Alternatively, for ePIV applications, the compounding of individual angles can be performed in the correlation domain [42], [43].

D. UCA concentration

The mean correlation values obtained during fast flow were much lower than during periods of slow flow, independent of UCA concentration. This was expected as more bubbles will exit (and enter) the interrogation region as the flow rate increases. Additional factors linked to flow speed, such as large flow gradients or out-of-plane flow can also reduce the correlation value obtained. There are methods to account for these effects: including the use of different size interrogation windows between frames; or the use of iterative block-matching schemes with window offset and/or deformation [29] (as was used to obtain the results in Fig. 9).

We found that high UCA concentrations facilitated higher correlation during low flow rates and vice versa. The reason for poor performance of low bubble concentrations during slow flow was likely the lower CBR during slow flow (Fig. 8b). The CBR decrease during slow flow was likely due to

more bubble destruction, caused by the increased ultrasound exposure time. Indeed, we observed distinct regions with signal loss, particularly during late diastole, which were more prominent in the 0.25 ml bolus data than in the 1.5 ml bolus data. Thus, for low concentrations, these signal drop-outs during slow flow may outweigh the small correlation improvements during fast flow, as the drop-outs result in significant tracking error.

The small correlation improvement gained by low UCA concentrations during fast flow is in agreement with *in vitro* studies using conventional line-scanning ultrasound for ePIV [21], [22]. Likely caused by less ‘particle-pairs’ being present in an interrogation window which reduces correlation uncertainty in the presence of strong flow gradients.

E. Limitations

This study did not test other non-linear contrast specific tissue suppression strategies, such as pulse inversion or power modulated pulse inversion (PMPI), which may have performed better with a different transducer. However, Desailly *et al.* reported similar results to this study when

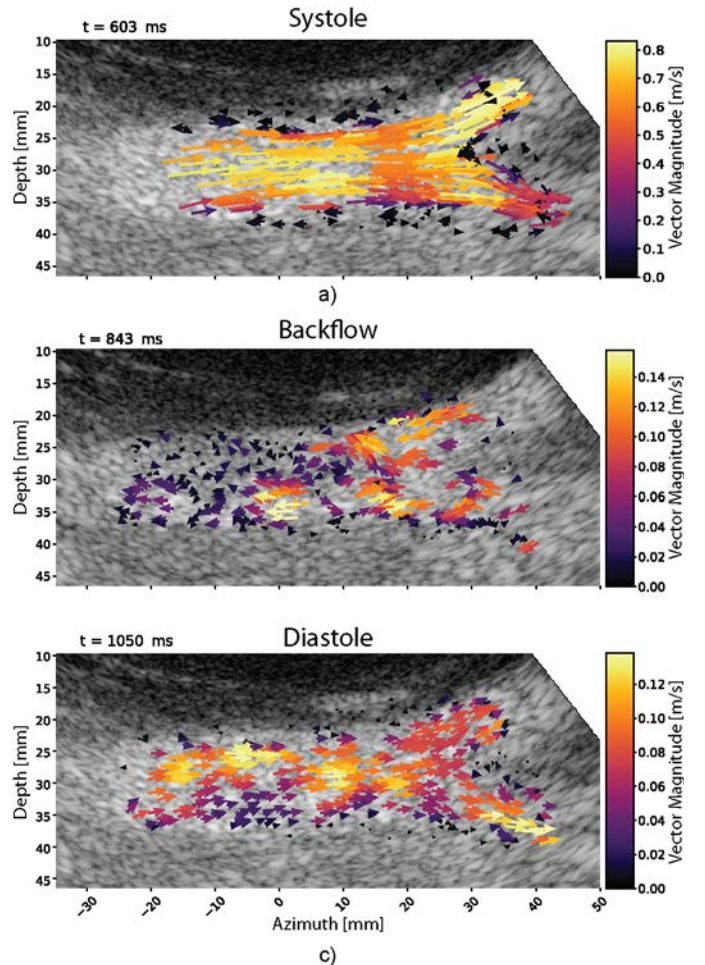


Fig. 9. ePIV derived velocity fields during three phases of the cardiac cycle: a) peak systole, b) backflow, and c) diastole. Results obtained with 0.01 MI, 1250 SVD ensembles and 1.5 ml UCA bolus.

comparing SVD with PMPI in a microvasculature environment [17].

The volunteers in this study had lower BMI than anticipated in the patients of interest, with relatively superficial aortas (32 ± 5 mm) compared with the depths that can be expected in patients (up to 100 mm, sometimes deeper). However, this preliminary study aimed to prove that HFR ePIV was possible in the region of the AA bifurcation, and to gain insight into optimal UCA parameters for future patient studies. The acoustic pressures required to obtain sufficient signal were also very low, thus the transmit power can be increased to obtain similar MIs in deeper regions. How ePIV is affected by the increased attenuation and reduced image quality in patients will be assessed in future studies.

We tested lower MIs only after discovering that the planned MI of 0.09 (derived from previous in-vitro studies) was causing severe bubble destruction *in vivo*. This forced a parameter adjustment for the following batches of volunteers, but allowed us to assess the influence of MI, which was beneficial for the final outcome. For future HFR CEUS studies, *in vivo*, one should be prepared to use very low MI, maybe even lower than the values used here.

The use of the normalized cross-correlation value as a surrogate for tracking performance is also a limitation of this study, although this is not uncommon [21]. This was required as reliable ground truth measurements were not feasible *in vivo*.

Finally, the PRF used in this study was not as high as physically possible, but was limited to keep spatial-peak temporal-average intensity (I_{SPTA}) under the recommended value for abdominal imaging [44]. We performed our I_{SPTA} safety measurements to allow for the maximum MI value tested, resulting in an I_{SPTA} value close to the 94 mW/cm^2 recommended for abdominal imaging. The use of the lower output pressures ($MI \leq 0.01$) in this study would allow for a higher PRF in future, possibly up to the physical maximum of $\sim 8000 \text{ Hz}$ at a depth of $\sim 10 \text{ cm}$.

V. CONCLUSION

We have shown that SVD can provide higher CBR than AM in the abdominal aorta, without requiring multiple transmissions per image. We found that lower MIs should be used *in vivo* to prevent bubble destruction, as compared to *in vitro* studies. Finally, we observed that higher UCA concentrations were associated with higher correlation during slow flow conditions and less signal drop-outs, but lower concentrations were associated with slightly higher correlation under fast flow conditions.

ACKNOWLEDGMENT

The authors thank Bastiaan Bongers (Rijnstate Hospital, Arnhem, the Netherlands) and Pavel Taimr MD (Erasmus MC, Rotterdam, the Netherlands) for their contribution to the high frame rate contrast enhanced ultrasound scans.

REFERENCES

- [1] D. E. Conway, M. R. Williams, S. G. Eskin, and L. V. McIntire, "Endothelial cell responses to atheroprone flow are driven by two separate flow components: low time-average shear stress and fluid flow reversal," *AJP Hear. Circ. Physiol.*, vol. 298, no. 2, pp. H367–H374, 2010.
- [2] A. Harloff, A. Nußbaumer, S. Bauer, A. F. Stalder, A. Frydrychowicz, C. Weiller, J. Hennig, and M. Markl, "In vivo assessment of wall shear stress in the atherosclerotic aorta using flow-sensitive 4D MRI," *Magn. Reson. Med.*, vol. 63, no. 6, pp. 1529–1536, Apr. 2010.
- [3] L. H. Timmins, D. S. Molony, P. Eshtehardi, M. C. McDaniel, J. N. Oshinski, D. P. Giddens, and H. Samady, "Oscillatory wall shear stress is a dominant flow characteristic affecting lesion progression patterns and plaque vulnerability in patients with coronary artery disease," *J. R. Soc. Interface*, vol. 14, no. 127, p. 20160972, Feb. 2017.
- [4] J. C. Lasheras, "The Biomechanics of Arterial Aneurysms," *Annu. Rev. Fluid Mech.*, vol. 39, no. 1, pp. 293–319, Jan. 2007.
- [5] J. T. Boersen, E. Groot Jebbink, M. Versluis, C. H. Slump, D. N. Ku, J.-P. P. M. de Vries, and M. M. P. J. Reijnen, "Flow and wall shear stress characterization after endovascular aneurysm repair and endovascular aneurysm sealing in an infrarenal aneurysm model," *J. Vasc. Surg.*, vol. 66, no. 6, pp. 1844–1853, Dec. 2017.
- [6] E. Groot Jebbink, V. Mathai, J. T. Boersen, C. Sun, C. H. Slump, P. C. J. M. Goverde, M. Versluis, and M. M. P. J. Reijnen, "Hemodynamic comparison of stent configurations used for aortoiliac occlusive disease," *J. Vasc. Surg.*, vol. 66, no. 1, pp. 251–260, 2017.
- [7] S. F. C. Stewart, "Effects of transducer, velocity, Doppler angle, and instrument settings on the accuracy of color Doppler ultrasound," *Ultrasound Med. Biol.*, vol. 27, no. 4, pp. 551–564, 2001.
- [8] J. A. Jensen, *Estimation of Blood Velocities Using Ultrasound, A Signal Processing Approach*. Cambridge University Press, 1996.
- [9] M. D. Fox, "Multiple crossed-beam ultrasound Doppler velocimetry," *IEEE Trans. Sonics Ultrason.*, vol. 25, no. 5, pp. 281–286, 1978.
- [10] P. Tortoli, M. Lenge, D. Righi, G. Ciuti, H. Liebgott, and S. Ricci, "Comparison of Carotid Artery Blood Velocity Measurements by Vector and Standard Doppler Approaches," *Ultrasound Med. Biol.*, vol. 41, no. 5, pp. 1354–1362, May 2015.
- [11] J. A. Jensen, S. I. Nikolov, J. Udesen, P. Munk, K. L. Hansen, M. M. Pedersen, P. M. Hansen, M. B. Nielsen, N. Oddershede, J. Kortbek, M. J. Pihl, and Y. Li, "Recent advances in blood flow vector velocity imaging," *IEEE Int. Ultrason. Symp. IUS*, pp. 262–271, 2011.
- [12] J. A. Jensen and P. Munk, "A new method for estimation of velocity vectors," *IEEE Trans. Ultrason. Ferroelectr. Freq. Control*, vol. 45, no. 3, pp. 837–851, May 1998.
- [13] J. A. Jensen, A. H. Brandt, and M. B. Nielsen, "Convex array vector velocity imaging using transverse oscillation and its optimization," *IEEE Trans. Ultrason. Ferroelectr. Freq. Control*, vol. 62, no. 12, pp. 2043–2053, 2015.
- [14] L. N. Bohs, B. H. Friemel, and G. E. Trahey, "Experimental velocity profiles and volumetric flow via two-dimensional speckle tracking," *Ultrasound Med. Biol.*, vol. 21, no. 7, pp. 885–898, Jan. 1995.
- [15] S. Fadnes, M. S. Wigen, S. A. Nyenes, and L. Lovstakken, "In Vivo Intracardiac Vector Flow Imaging Using Phased Array Transducers for Pediatric Cardiology," *IEEE Trans. Ultrason. Ferroelectr. Freq. Control*, vol. 64, no. 9, pp. 1318–1326, Sep. 2017.
- [16] J. Voorneveld, P. Kruizinga, H. J. Vos, F. J. H. Gijzen, E. G. Jebbink, A. F. W. van der Steen, N. de Jong, and J. G. Bosch, "Native blood speckle vs ultrasound contrast agent for particle image velocimetry with ultrafast ultrasound - in vitro experiments," in *2016 IEEE International Ultrasonics Symposium (IUS)*, 2016.
- [17] Y. Desailly, A.-M. Tissier, J.-M. Correas, F. Wintzenrieth, M. Tanter, and O. Couture, "Contrast enhanced ultrasound by real-time

- spatiotemporal filtering of ultrafast images,” *Phys. Med. Biol.*, vol. 62, no. 1, pp. 31–42, 2017.
- [18] O. Couture, M. Fink, and M. Tanter, “Ultrasound contrast plane wave imaging,” *IEEE Trans. Ultrason. Ferroelectr. Freq. Control*, vol. 59, no. 12, pp. 2676–2683, 2012.
- [19] C. Tremblay-Darveau, R. Williams, L. Milot, M. Bruce, and P. N. Burns, “Combined perfusion and doppler imaging using plane-wave nonlinear detection and microbubble contrast agents,” *IEEE Trans. Ultrason. Ferroelectr. Freq. Control*, vol. 61, no. 12, pp. 1988–2000, 2014.
- [20] M. Toulemonde, R. J. Eckersley, and M.-X. Tang, “High frame rate contrast enhanced echocardiography: Microbubbles stability and contrast evaluation,” in *IEEE International Ultrasonics Symposium (IUS)*, 2017.
- [21] L. Liu, H. Zheng, L. Williams, F. Zhang, R. Wang, J. Hertzberg, and R. Shandas, “Development of a custom-designed echo particle image velocimetry system for multi-component hemodynamic measurements: system characterization and initial experimental results,” *Phys. Med. Biol.*, vol. 53, no. 5, pp. 1397–1412, 2008.
- [22] H. B. Kim, J. R. Hertzberg, and R. Shandas, “Development and validation of echo PIV,” *Exp. Fluids*, vol. 36, no. 3, pp. 455–462, 2004.
- [23] S. A. J. Engelhard, J. Voorneveld, H. J. Vos, J. J. M. Westenberg, F. J. H. Gijzen, P. Taimr, M. Versluis, N. de Jong, J. G. Bosch, M. M. P. J. Reijnen, and E. Groot Jebbink, “High-Frame-Rate Contrast Enhanced US Particle Image Velocimetry in the Abdominal Aorta: first human results.” *Radiology*, in press, doi: <https://doi.org/10.1148/radiol.2018172979>.
- [24] G. A. Brock-Fisher, M. D. Poland, and P. G. Rafter, “Means for increasing sensitivity in non-linear ultrasound imaging systems,” 5 577 505 A, 1996.
- [25] T. A. Whittingham, “Contrast-Specific Imaging Techniques: Technical Perspective,” in *Contrast Media in Ultrasonography*, Berlin/Heidelberg: Springer-Verlag, 2005, pp. 43–70.
- [26] C. Demene, T. Deffieux, M. Pernot, B.-F. Osmanski, V. Biran, J.-L. Gennisson, L.-A. Sieu, A. Bergel, S. Franqui, J.-M. Correas, I. Cohen, O. Baud, and M. Tanter, “Spatiotemporal Clutter Filtering of Ultrafast Ultrasound Data Highly Increases Doppler and fUltrasound Sensitivity,” *IEEE Trans. Med. Imaging*, vol. 34, no. 11, pp. 2271–2285, Nov. 2015.
- [27] A. Yu and L. Lovstakken, “Eigen-based clutter filter design for ultrasound color flow imaging: a review,” *IEEE Trans. Ultrason. Ferroelectr. Freq. Control*, vol. 57, no. 5, pp. 1096–1111, May 2010.
- [28] J. Viti, H. Vos, N. De Jong, F. Guidi, and P. Tortoli, “Detection of Contrast Agents: Plane Wave vs Focused Transmission,” *IEEE Trans. Ultrason. Ferroelectr. Freq. Control*, vol. 63, no. 2, pp. 203–211, 2016.
- [29] R. J. Adrian and J. Westerweel, *Particle Image Velocimetry*. Cambridge University Press, 2011.
- [30] B. Y. S. Yiu, S. S. M. Lai, and A. C. H. Yu, “Vector Projectile Imaging: Time-Resolved Dynamic Visualization of Complex Flow Patterns,” *Ultrasound Med. Biol.*, vol. 40, no. 9, pp. 2295–2309, 2014.
- [31] F. A. Duck, “Nonlinear acoustics in diagnostic ultrasound,” *Ultrasound Med. Biol.*, vol. 28, no. 1, pp. 1–18, Jan. 2002.
- [32] M. Tang and R. Eckersley, “Nonlinear propagation of ultrasound through microbubble contrast agents and implications for imaging,” *IEEE Trans. Ultrason. Ferroelectr. Freq. Control*, vol. 53, no. 12, pp. 2406–2415, Dec. 2006.
- [33] G. L. ten Kate, G. G. J. Renaud, Z. Akkus, S. C. H. van den Oord, F. J. ten Cate, V. Shamdassani, R. R. Entrekin, E. J. G. Sijbrands, N. de Jong, J. G. Bosch, A. F. L. Schinkel, and A. F. W. van der Steen, “Far-Wall Pseudoenhancement During Contrast-Enhanced Ultrasound of the Carotid Arteries: Clinical Description and In Vitro Reproduction,” *Ultrasound Med. Biol.*, vol. 38, no. 4, pp. 593–600, Apr. 2012.
- [34] J. S. Lum, D. M. Stobbe, T. W. Murray, and M. A. Borden, “Single microbubble measurements of temperature dependent viscoelastic properties,” in *2017 IEEE International Ultrasonics Symposium (IUS)*, 2017.
- [35] H. Mulvana, E. Stride, J. V. Hajnal, and R. J. Eckersley, “Temperature Dependent Behavior of Ultrasound Contrast Agents,” *Ultrasound Med. Biol.*, vol. 36, no. 6, pp. 925–934, Jun. 2010.
- [36] H. J. Vos, M. Emmer, and N. de Jong, “Oscillation of single microbubbles at room versus body temperature,” in *2008 IEEE Ultrasonics Symposium*, 2008, pp. 982–984.
- [37] A. A. Brayman, M. Azadniv, M. W. Miller, and R. S. Meltzer, “Effect of static pressure on acoustic transmittance of Albnex (R) microbubble suspensions,” *J. Acoust. Soc. Am.*, vol. 99, no. 4, pp. 2403–2408, Apr. 1996.
- [38] M. Itani and R. F. Mattrey, “The Effect of Inhaled Gases on Ultrasound Contrast Agent Longevity In Vivo,” *Mol. Imaging Biol.*, vol. 14, no. 1, pp. 40–46, Feb. 2012.
- [39] J. J. Kwan and M. A. Borden, “Microbubble Dissolution in a Multigas Environment,” *Langmuir*, vol. 26, no. 9, pp. 6542–6548, May 2010.
- [40] G. Montaldo, M. Tanter, J. Bercoff, N. Benech, and M. Fink, “Coherent plane-wave compounding for very high frame rate ultrasonography and transient elastography,” *IEEE Trans. Ultrason. Ferroelectr. Freq. Control*, vol. 56, no. 3, pp. 489–506, 2009.
- [41] B. Denarie, T. A. Tangen, I. K. Ekroll, N. Rolim, H. Torp, T. Bjastad, and L. Lovstakken, “Coherent plane wave compounding for very high frame rate ultrasonography of rapidly moving targets,” *IEEE Trans. Med. Imaging*, vol. 32, no. 7, pp. 1265–1276, 2013.
- [42] C. H. Leow and M.-X. Tang, “Spatio-Temporal Flow and Wall Shear Stress Mapping Based on Incoherent Ensemble-Correlation of Ultrafast Contrast Enhanced Ultrasound Images,” *Ultrasound Med. Biol.*, vol. 44, no. 1, pp. 134–152, Jan. 2018.
- [43] J. Voorneveld, A. Muralidharan, T. Hope, H. J. Vos, P. Kruizinga, A. F. W. van der Steen, F. J. H. Gijzen, S. Kenjeres, N. de Jong, and J. G. Bosch, “High Frame Rate Ultrasound Particle Image Velocimetry for Estimating High Velocity Flow Patterns in the Left Ventricle,” *IEEE Trans. Ultrason. Ferroelectr. Freq. Control*, pp. 1–1, 2017.
- [44] US Food and Drug Administration, *Information for Manufacturers Seeking Marketing Clearance of Diagnostic Ultrasound Systems and Transducers*. 2008.



Jason Voorneveld was born in Johannesburg, South Africa in 1987. He received his B.Sc. in Electro-Mechanical Engineering from the University of Cape Town, Cape Town, South Africa, in 2009. He then worked as a maintenance/project engineer at Indigo Brands, Cape Town, South Africa, from 2009-2013, before returning to complete his M.Sc. in Biomedical Engineering at the University of Cape Town in 2014. He is currently pursuing his Ph.D. in Biomedical Engineering at Erasmus MC, Rotterdam, the Netherlands. His research interests include high frame rate ultrasound imaging, blood flow imaging and ultrasound image/signal processing.



Stefan Engelhard was Born in Oirschot, the Netherlands in 1990. He received the BSc and MSc degrees in Technical Medicine (track: Medical Sensing and Stimulation) from the University of Twente, Enschede, in 2016. He is currently working as a clinical researcher and Phd candidate in the Rijnstate

Hospital in Arnhem, focusing on in-vivo US-based bloodflow measurements.



Hendrik J. Vos received the M.Sc. degree in Applied Physics from Delft University of Technology, Delft, The Netherlands in 2004, and his Ph.D. degree with the Department of Biomedical Engineering at Erasmus MC, Rotterdam, The Netherlands, in 2010. He currently is assistant professor with Erasmus MC, and received a Dutch NWO-TTW-VIDI personal grant in 2018. His research interests include medical 2D and 3D high frame rate imaging of shear waves and contrast agents.



Michel Reijnen (MD, PHD), born June 3 1971, finished his (endo)vascular training in January 2004 and joined the Rijnstate Hospital in Arnhem, the Netherlands in 2007, where he works in a team of 5 vascular surgeons and 4 interventional radiologists. He is involved in multiple trials in the endovascular area and initiator and principal investigator of various (inter)national multicentre randomized trials and Registries. There is a close collaboration with the University of Twente, Enschede, The Netherlands, in the field of Vascular Imaging and Innovation. He published over 150 peer reviewed manuscripts and book chapters and is reviewer of several journals and a regular faculty member of several international symposia. Being the course director of surgical residents until 2017 and having organized multiple workshops in the endovascular field, he has a profound interest and experience in surgical training.



Frank Gijzen obtained his Ph.D. at the Eindhoven University of Technology, Eindhoven, the Netherlands, with a thesis on the modelling of blood flow in large arteries. After his PhD he was founder of a bioengineering company, and he was involved as a board member in setting up the department of Biomedical Engineering at the Eindhoven University of Technology in Eindhoven. He moved to the Erasmus MC in 2001, where he started as a post-doc and currently serves as associate professor in the Department of Biomedical Engineering of the Thorax Center, Erasmus MC, Rotterdam. He is (co-)author of approximately 80 scientific papers, 6 book chapters, and he recently served as a guest editor for a special issue on 'Plaque Mechanics' for the journal of Biomechanics. He is the recipient of national and international grants and one of the founders and organizers of the international symposium on Biomechanics in Vascular

Biology and Cardiovascular Disease. His research covers image-based biomechanics of the cardiovascular system. His research interests include the influence of blood flow induced wall shear stress on plaque progression, composition, stability and rupture.



Michel Versluis was born in The Netherlands in 1963. He graduated with a degree in physics in 1988 from the University of Nijmegen, The Netherlands, with a special interest in molecular physics and astrophysics, working in the field of far-infrared laser spectroscopy of interstellar molecular species. Later, he specialized in the application of intense tunable ultraviolet lasers for flame diagnostics, resulting in a successful defense of his PhD thesis in 1992. After a two-year research position working on molecular dynamics at Griffith University, Brisbane, Australia, he continued to work on developing laser diagnostic techniques for internal combustion engines (Lund, Sweden) and industrial jet flames and solid rocket propellants (Delft, The Netherlands). Dr. Versluis is now full professor Physical and Medical Acoustics at the University of Twente, The Netherlands, in the Physics of Fluids group. He is an expert in ultra-high-speed imaging with a particular interest in the use of microbubbles and microdroplets for medical applications, both in imaging and in therapy, and in the physics and control of bubbles and droplets in microfluidic applications in medicine and the nanotechnology industry.



Erik Groot Jebbink (1987) received the B.S. (2009) and M.S. (2013) degrees in Technical Medicine from the University of Twente, Enschede, The Netherlands. In 2017 he obtained his Ph.D. degree at the Physics of Fluids group, University of Twente. From 2018 on he has a postdoc position at the M3i group, University of Twente, and a part-time appointment at the department of Vascular Surgery at the Rijnstate hospital, Arnhem. His research interests focus on the interaction between blood flow and stents, based on in vitro and in vivo measurements.



Nico de Jong received the M.Sc. degree in physics specialized in the field of pattern recognition from Delft University of Technology, Delft, The Netherlands, in 1978, and the Ph.D. degree with a specialization in acoustic properties of ultrasound contrast agents in 1993 from the Department of Biomedical

Engineering, Thorax Center, Erasmus MC, The Netherlands. In 2003, he joined the University of Twente, Enschede, the Netherlands, as a part-time Professor. He currently teaches with Technical Universities and Erasmus MC. He has been a Promotor of 21 Ph.D. students and is currently co-supervising 11 Ph.D. students. Since 1980, he has been a Staff Member with the Thorax Center, Erasmus Medical Center (Erasmus MC), Rotterdam, The Netherlands. Since 2011, he has been a Professor of Molecular Ultrasonic Imaging and Therapy with Erasmus MC and the Delft University of Technology, and since 2015, he has been the part-time Head of the Department of Acoustical Waveform Imaging with the Delft University of Technology.

Over the last 5 years, he has given more than 30 invited lectures and has given numerous scientific presentations for international industries. He has authored 260 peer-reviewed articles and has been a Principal Investigator (PI) and the Workpackage Leader of the European and Dutch projects. His H-factor is 46 (Web of science), and he has been acquired more than 6 M€ as a PI or a Co-PI since 2010. Dr. Jong is the Organizer of the Annual European Symposium on Ultrasound Contrast Imaging, Rotterdam, which is attended by approximately 175 scientists from universities and industries all over the world. He is on the Safety Committee of the World Federation of *Ultrasound in Medicine and Biology*, and is an Associate Editor of *Ultrasound in Medicine and Biology*, and a Guest Editor of the special issues of different journals.



Johan G. Bosch is an Associate Professor and staff member at the Department of Biomedical Engineering, Thoraxcenter, Erasmus MC, Rotterdam. He is specialized in 2D and 3D echocardiographic image processing/analysis and transducer development. Main research interests are optimal border detection approaches,

geometrical and statistical models, and anatomical and physical knowledge representations for border detection. He is currently leader of projects on 3D segmentation and 3D ultrasound guidance in electrophysiology and participates in several projects, e.g. on 3D transducer development, 2D and 3D carotid imaging, and 3D TEE imaging.

He obtained his MSc in Electrical Engineering at Eindhoven University of Technology in 1985. He performed ultrasound and image processing research at Erasmus University Rotterdam and Leiden University. From 1995-2005, he was Assistant Professor and head of the Echocardiography section at the Division of Image Processing (LKEB), Department of Radiology, Leiden University Medical Center, where he obtained his PhD in 2006.